



Design and Fabrication of Aperiodic Multilayers with  
Broadband Reflectance in the Soft X-ray regime

Jirawit Ratanapreechachai  
University of Cambridge, United Kingdom

Deutsches Elektronen-Synchrotron (DESY)  
July 22, 2014 – September 11, 2014

## Abstract

Aperiodic multilayer structures have been designed for broadband reflectance in the soft X-ray region by MATLAB-based codes. The codes were first written to calculate the reflectivity response of any arbitrary multilayer structure taking into account the effects of interface imperfections and then developed further to solve the inverse problem of finding the layer thicknesses of an aperiodic multilayer structure that will give the desired reflectivity response. The Luus-Jaakola optimisation algorithm was employed to find the optimal design by minimising the figure of merit. As a result, the optimised designs were obtained for the Molybdenum/Silicon and Scandium/Chromium systems with top-flat reflectivity responses between 17 and 22 nm and between 4.30 and 4.42 nm respectively at a fixed incidence angle of  $5^\circ$  from the normal. For the Molybdenum/Silicon system, aperiodic multilayers were fabricated according to the optimised design and characterised by X-ray diffraction measurements. The measured diffraction pattern has the same overall appearance as the computational prediction for the optimised structure. This proves that the deposition process used is able to fabricate aperiodic multilayers according to the optimised design to high accuracy. For the Scandium/Chromium system, it has been known that aperiodic multilayers with 100 bilayers are able to achieve a reflectivity of about 1 % over an energy range of about 300–350 eV at a fixed incidence angle of  $45^\circ$ . By using our developed algorithms, the optimised layer thicknesses of such a multilayer were found successfully according to the specified broadband reflectivity response as an attempt to replicate the given results.

# Contents

<b>1</b>	<b>Introduction</b>	<b>1</b>
<b>2</b>	<b>Theoretical Background</b>	<b>1</b>
2.1	Multilayer Reflectivity Calculation . . . . .	1
2.1.1	Ideal Case . . . . .	1
2.1.2	Interface Imperfections . . . . .	3
2.2	Inverse Problem . . . . .	5
2.2.1	Figure of Merit . . . . .	6
<b>3</b>	<b>Computational Methods</b>	<b>6</b>
3.1	Reflectivity Simulation . . . . .	6
3.2	Optimisation Procedure . . . . .	7
3.3	Fabrication & Characterisation . . . . .	8
<b>4</b>	<b>Results &amp; Discussions</b>	<b>9</b>
4.1	Preliminary Checks . . . . .	9
4.2	Non-ideal Interfacial Effects . . . . .	9
4.3	Optimisation Results . . . . .	13
4.3.1	Molybdenum/Silicon Multilayer System . . . . .	13
4.3.2	Scandium/Chromium Multilayer System . . . . .	13
4.4	Comparison with Measurements . . . . .	13
4.4.1	Hard X-ray Diffraction Measurements . . . . .	13
4.4.2	Soft X-ray Reflectivity Measurements . . . . .	16
<b>5</b>	<b>Further Discussions</b>	<b>16</b>
5.1	Potential Applications . . . . .	16
5.2	Improvements to the Program . . . . .	18
<b>6</b>	<b>Conclusions</b>	<b>18</b>

# 1 Introduction

A typical multilayer structure is composed of a stack of alternating layers of two optically different materials. Such a structure is able to achieve a high reflectivity in the soft X-ray region, which is difficult to achieve in bulk materials. Periodic multilayers are ones in which the layer thickness of each material remains constant throughout the stack. On the other hand, aperiodic multilayers are ones in which the layer thickness varies along the structure. Typically, the bandwidth of a periodic multilayer is small. An effective way to increase the bandwidth is to use aperiodic multilayers.

Designing aperiodic multilayers is a difficult optimisation problem due to the large number of independent parameters. The Luus-Jaakola optimisation algorithm is a potential candidate that may enable the optimisation problem to be solved efficiently. The goals of this paper are to find an effective method to design aperiodic multilayers subject to broadband reflectivity profiles, which will be used in future experiments, familiarise with the ongoing research field of multilayer X-ray optics and understand the working mechanism of an aperiodic multilayer, along with its fabrication procedure.

In this paper, the theoretical simulations and the broadband aperiodic multilayer designs for ... are presented. The theoretical background of multilayer X-ray optics is summarised in Section 2. Section 3 deals with the computational methods including the optimisation algorithm. The optimisation results and the performance of the algorithm are then discussed in Section 4. Finally, the conclusions are given in Section 6.

## 2 Theoretical Background

### 2.1 Multilayer Reflectivity Calculation

#### 2.1.1 Ideal Case

A generalised multilayer structure is depicted in Figure 1. Each layer is characterised by its location,  $j$ , in the stack, its layer thickness  $t_j$  and its complex refractive index  $n_j$ .  $\lambda$  is the incident radiation wavelength.

In the soft X-ray region, the complex refractive index  $n$  of a material is conventionally written in the form

$$n = 1 - \delta - i\beta,$$

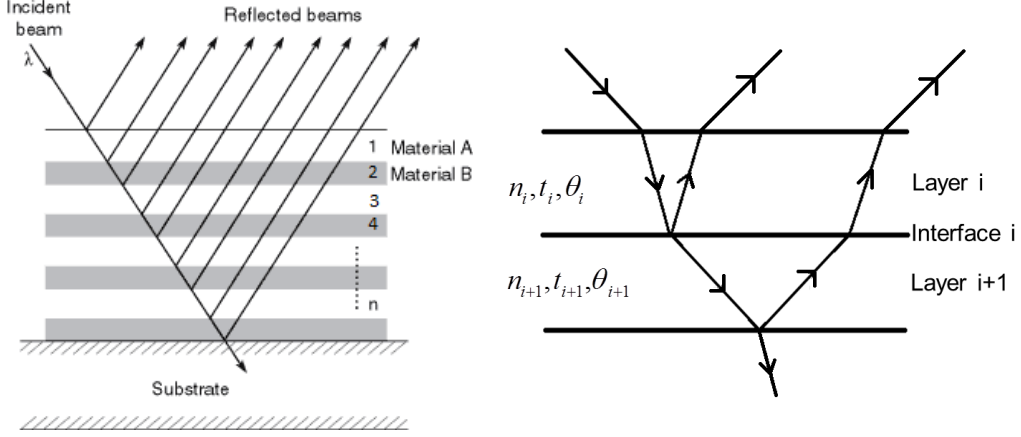


Figure 1: Schematic diagram showing the reflections from a general multi-layer structure (left) and the notation used in the text (right).

where  $\delta$  and  $\beta$  are real and usually  $\delta, \beta \ll 1$ .

For s-polarised radiation, where the electric field vector is perpendicular to the plane of incidence, the Fresnel reflection coefficient for the  $j^{\text{th}}$  interface between layers  $j$  and  $j + 1$  is given by

$$r_{j,j+1}^s = \frac{n_j \cos \theta_j - n_{j+1} \cos \theta_{j+1}}{n_j \cos \theta_j + n_{j+1} \cos \theta_{j+1}}. \quad (1)$$

Similarly for p-polarised radiation, where the electric field vector is parallel to the plane of incidence,

$$r_{j,j+1}^p = \frac{n_j \cos \theta_{j+1} - n_{j+1} \cos \theta_j}{n_j \cos \theta_{j+1} + n_{j+1} \cos \theta_j}. \quad (2)$$

Here,  $\theta_j$  refers to the complex angle of propagation in the  $j^{\text{th}}$  layer, which is governed by Snell's law,

$$n_j \cos \theta_j = \sqrt{n_j^2 - \sin^2 \theta},$$

where  $\theta$  is the angle of incidence at the top of the structure measured from the normal.

The recursion relation for the total reflected amplitude from the  $j^{\text{th}}$  interface ( $\chi_j$ ) is given by

$$\chi_j = \frac{r_{j,j+1} + \chi_{j+1} \exp(-i2\phi_{j+1})}{1 + r_{j,j+1}\chi_{j+1} \exp(-i2\phi_{j+1})}, \text{ where } \phi_j = \frac{2\pi}{\lambda} t_j n_j \cos \theta_j. \quad (3)$$

The recursion is started from the bottom of the structure by assuming that there is no reflection from the back of the semi-infinite substrate, i.e.,  $\chi_{2N+1} = 0$ , where  $N$  is the total number of bilayers. Hence,  $\chi_0$  can be found by solving Eq. 3 recursively. The net reflectance for the multilayer stack is then obtained from  $|\chi_0|^2$ .

Moreover, as the Fresnel reflection coefficients for s and p polarisations are different (Eqs. 1 and 2). All the calculations must be done separately for each polarisation. By first defining the polarisation factor  $f$  of the incident radiation as

$$f = \frac{I^s - I^p}{I^s + I^p},$$

where  $I^s$  and  $I^p$  are the incident intensities for s and p polarisations respectively, the polarisation average reflectance  $R^a$  can be written as

$$R^a = \frac{R^s(1 + f) + R^p(1 - f)}{2}. \quad (4)$$

Note that unpolarised radiation corresponds to  $f = 0$  and Eq. 4 reduces to the usual average  $R^a = \frac{R^s + R^p}{2}$ .

### 2.1.2 Interface Imperfections

The above formulae are valid based on the assumption that interfaces between different materials are perfectly flat and infinitely sharp. In reality, we need to take into account interface imperfections which can be roughness, diffuseness or a combination of the two effects. As a result, the interface imperfections lead to an overall decrease in the specular reflectance.

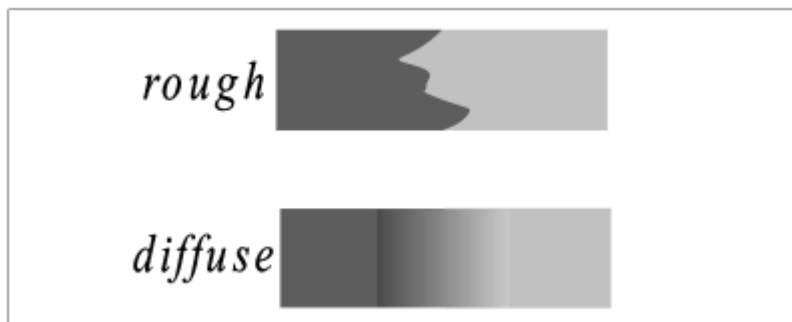


Figure 2: Schematic illustration of purely rough and purely diffuse interfaces.

**Interface Roughness** When an electromagnetic radiation is incident on a rough interface (Figure 3), the radiation is scattered into other directions as well as reflected at the interface. Hence, the reflection from a rough interface is lower than that from a perfectly smooth interface.

There are various approaches to model the reduction in the specular reflectance due to interfacial roughness. Following the formalism by Stearns, the resultant loss in the specular reflectance can be approximated by multiplying the Fresnel reflection coefficients by a Névot-Croce roughness factor of the form

$$F_{j,j+1} = \exp \left[ -\frac{8\pi^2}{\lambda^2} (n_j \cos \theta_j)(n_{j+1} \cos \theta_{j+1})\sigma^2 \right],$$

where  $\sigma$  is the root-mean-square (rms) interfacial roughness. Therefore,

$$r'_{j,j+1} \equiv r_{j,j+1} F_{j,j+1}.$$

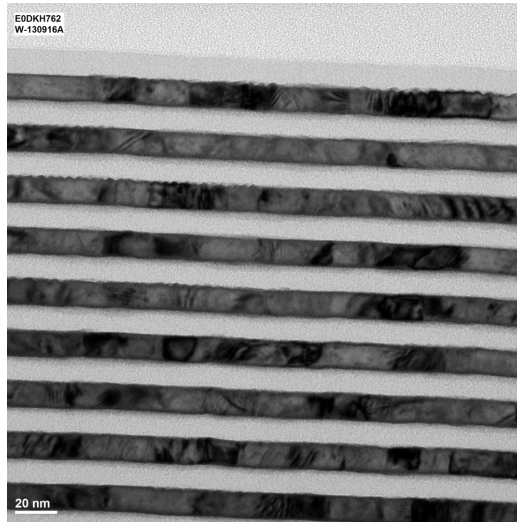


Figure 3: TEM image of a SiC/W multilayer showing interfacial roughness.

**Interface Diffusion** The diffusive mixing of the two materials in contact in a multilayer structure causes the corresponding interface to appear “diffuse” (Figure 5).

The above formalism for a rough interface can be applied equally well to a diffuse interface. However, a simplified approach has been used instead to describe the effects of interface diffusion. This approach treats a diffuse interface effectively as another layer located between any pair of layers (Figure

4). The thickness of this so called interfacial layer is usually characterised by the properties of the two multilayer components only and independent of the thicknesses of the surrounding layers.

In the case of the Mo/Si multilayer system, the interface layers are composed of  $\text{MoSi}_2$  (Figure 5), which has a thickness of 1.2 nm if Mo is on top of Si and 0.8 nm if Si is on top of Mo.

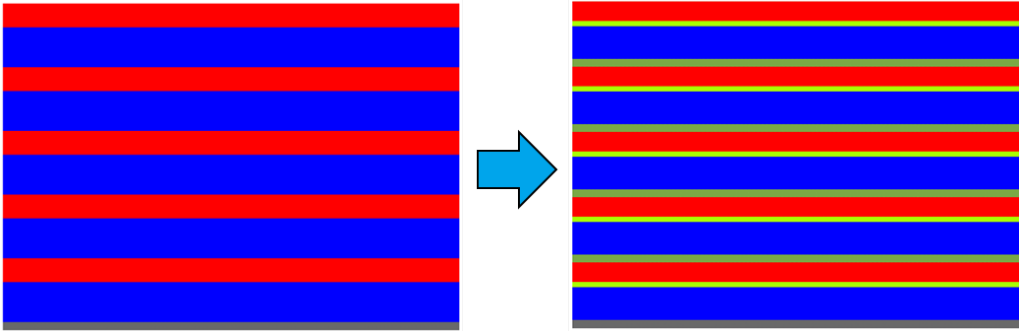


Figure 4: Schematic diagram showing how to insert an interfacial layer.

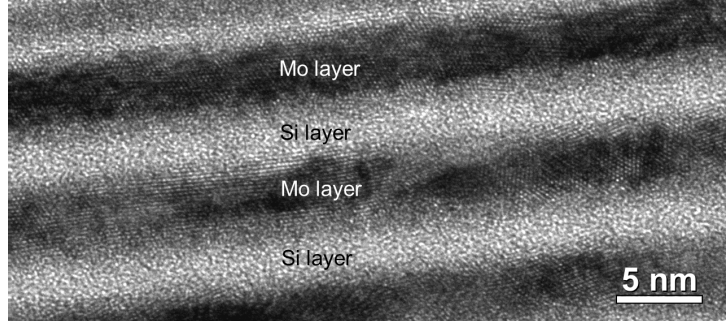


Figure 5: TEM image of a Mo/Si multilayer showing the forming of  $\text{MoSi}_2$  interfacial layers.

## 2.2 Inverse Problem

If the layer thicknesses of a multilayer structure are known, it is relatively straightforward to solve Eq. 3 recursively to find the specular reflectivity. However, the inverse problem of finding the layer thicknesses of a multilayer structure with a given reflectivity profile is more complicated and has no exact



analytic solutions. Therefore, numerical optimisation methods are needed in order to find the multilayer structure with the reflectivity response closest to the desired target.

### 2.2.1 Figure of Merit

In order to find the optimised multilayer structure, it is beneficial to define a numerical measure that will quantify the agreement between the current reflectivity and the target reflectivity responses. This quantity is termed the figure of merit (FOM) and given by,

$$FOM = \frac{\sum_i^S |R(\lambda_i) - R_0(\lambda_i)|}{S},$$

where S is the total number of data points within the considered wavelength region.

Therefore, the problem of finding the optimised layer thicknesses of a multilayer translates to the problem of minimising the figure of merit subject to the layer thicknesses. Also, we aim to reach the global minimum or at least a sufficiently deep local minimum so that there is a good agreement between the optimised and target reflectivity responses. This can be achieved by numerical optimisation methods of your choice.

## 3 Computational Methods

### 3.1 Reflectivity Simulation

Computational codes, based on MATLAB, were first developed to calculate the specular reflectivity for an arbitrary multilayer structure, either periodic or aperiodic, according to the basic equations described in Section 2. This was done for all the three interfacial properties: perfect, rough and diffuse.<sup>1</sup>. The reflectivity simulations generated by the codes were compared with those calculated by IMD<sup>2</sup> for both periodic Mo/Si and Sc/Cr structures as a preliminary check for the correctness and reliability of the developed codes.

---

<sup>1</sup>In fact, there is also a case where an interface is both rough and diffuse. However, this is not within the scope of this paper

<sup>2</sup>IMD is a software for simulating the optical properties of multilayer films developed by David Windt

In the Mo/Si system, the effect of interfacial roughness is negligible and the interfaces between different materials can be treated as purely diffuse by adding a MoS

In contrast, there is negligible interface diffusion in the Sc/Cr system and the interfaces can be treated as purely rough by multiply by th

## 3.2 Optimisation Procedure

The Luus-Jaakola optimisation method was employed to find the design which minimises the figure of merit. The MATLAB code from Section 3.1 was extended to follow the following scheme:

1. Start with an initial “parent” multilayer structure. It can be any reasonable structure and it is chosen to be a periodic multilayer in the paper for simplicity.
2. Choose an appropriate initial thickness variation size.
3. Introduce random thickness variations to the parent multilayer in order to generate a set of  $R$  “child” aperiodic multilayers.
4. Calculate the reflectivity and hence the figure merit of each child multilayer
5. Choose the child with the smallest figure of merit to be the new parent multilayer for the next iteration
6. Repeat steps 2–4  $I$  times.
7. Reduce the size of the random variations by a certain factor.
8. Repeat steps 2–6  $P$  times until the thickness variations are small enough to get the optimised aperiodic multilayer for a given reflectivity response

Note that  $R, I, P$  are positive integers. The above steps are summarised in Figure 6.

Although the layer thickness is changed randomly during the process, the upper and lower limits need to be set on the layer thickness in order to avoid having unphysical thick or thin layers in the final structure. The limits were

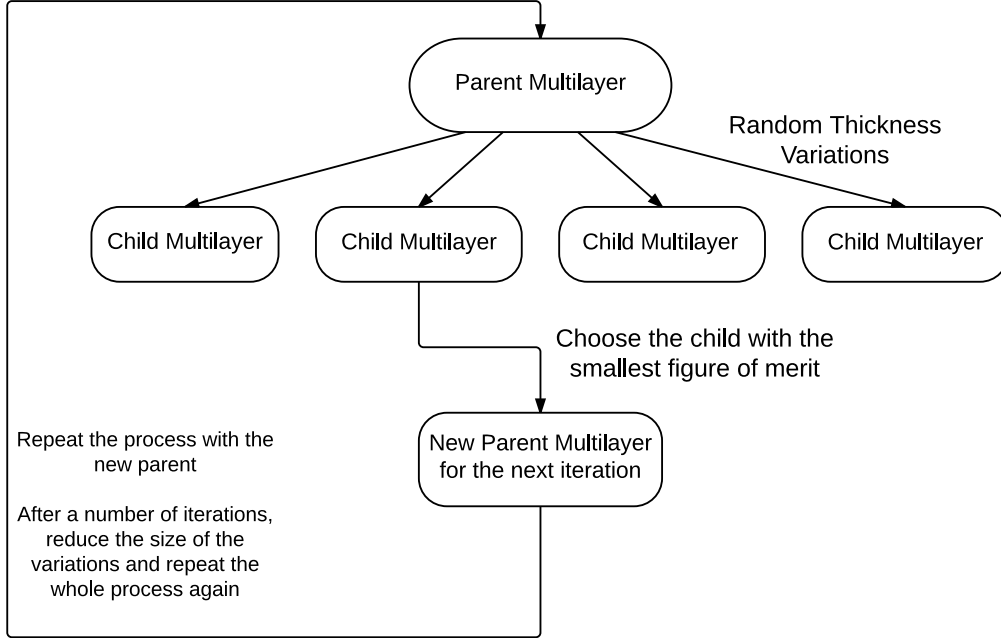


Figure 6: Flow chart demonstrating the Luus-Jaakola optimisation algorithm.

from 2 to 10 nm for the Mo/Si system and from 0.3 and 3.0 nm for the Sc/Cr system.

Equivalently, we are considering random points located within a sphere centred at the parent multilayer with the radius equal to the size of the thickness variation in  $2N$  dimensions.

### 3.3 Fabrication & Characterisation

Aperiodic multilayers were fabricated using direct current magnetron sputtering in the X-ray multilayer laboratory at Deutsches Elektronen-Synchrotron (DESY). The sputtering system consists of four magnetrons at the top of the vacuum chamber. They are spaced by  $90^\circ$  in a sputter-upward configuration. In the deposition process, Si and Mo targets were located  $180^\circ$  apart. A superpolished 2-inch Si (100) wafer was used as the substrate, which was then mounted on a rotating platter below the sputtering sources. The thicknesses of the deposited layers were controlled by modulating the platter velocity.

To achieve better thickness uniformity, the substrate was also spun around its own axis.

The fabricated aperiodic multilayers were then characterised with the lab-based X-ray diffractometer, which measures the reflectance as a function of grazing incidence angle, equipped with Cu  $K_\alpha$  X-ray sources (about 8 keV). The resulting diffraction pattern gives information on the quality of the layers of a multilayer structure.

## 4 Results & Discussions

### 4.1 Preliminary Checks

The reflectivity simulations produced from the codes were compared with those from IMD for various structures as follows:

- periodic Mo/Si multilayer with  $N = 20$ , period = 7.0 nm, Mo-to-Si thickness ratio of 1:1 and no interface imperfections (Figure 7)
- periodic Mo/Si multilayer with  $N = 20$ , period = 7.0 nm, Mo-to-Si thickness ratio of 1:1 and interface diffusion (Figure 8)
- periodic Sc/Cr multilayer with  $N = 200$ , period = 2.2 nm, Sc-to-Cr thickness ratio of 1:1 and no interface imperfections (Figure 9)
- periodic Sc/Cr multilayer with  $N = 200$ , period = 2.2 nm, Sc-to-Cr thickness ratio of 1:1 and interface roughness of 0.3 nm (Figure 10)

From these plots, it was clear that the simulations from our codes were consistent those from IMD in every case to very high accuracy. Therefore, the codes should be used as a basis for the figure of merit evaluation in subsequent optimisation steps.

### 4.2 Non-ideal Interfacial Effects

The effects of interface imperfections were investigated and the results for each case were shown below.

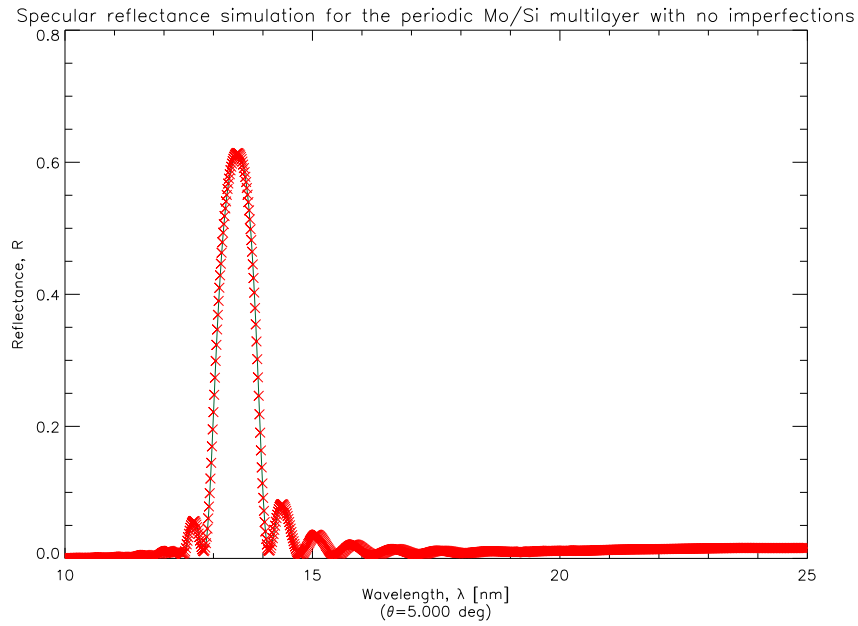


Figure 7: Specular reflectivity of a periodic 20-bilayer Mo/Si multilayer with no interface imperfections at a fixed incidence angle of  $5^\circ$  from the normal.

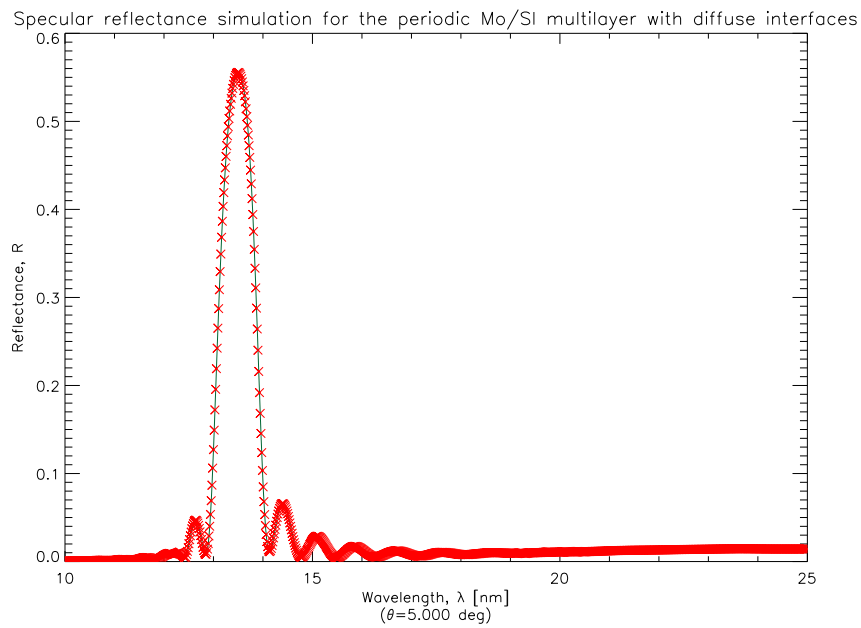


Figure 8: Specular reflectivity of a periodic 20-bilayer Mo/Si multilayer with interface diffusion at a fixed incidence angle of  $5^\circ$  from the normal.

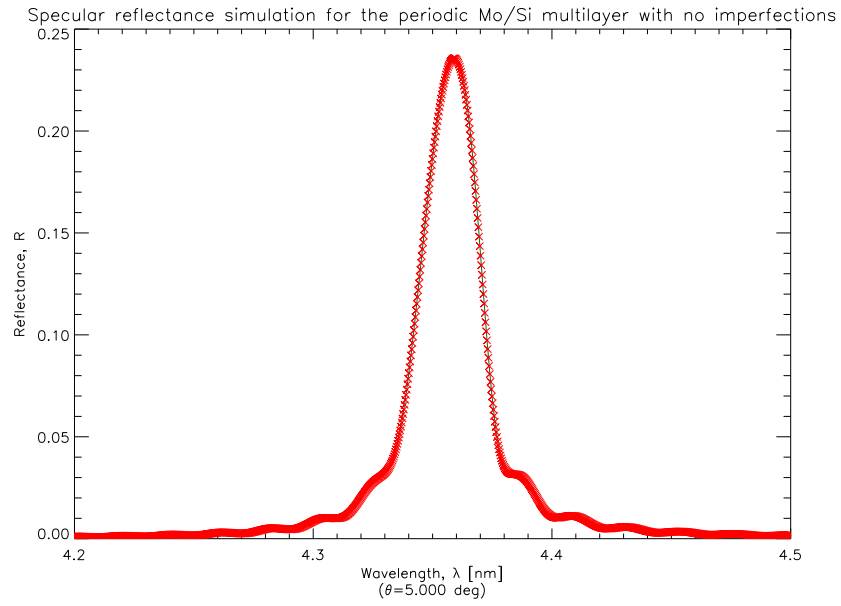


Figure 9: Specular reflectivity of a periodic 200-bilayer Sc/Cr multilayer with no interface imperfections at a fixed incidence angle of  $5^\circ$  from the normal.

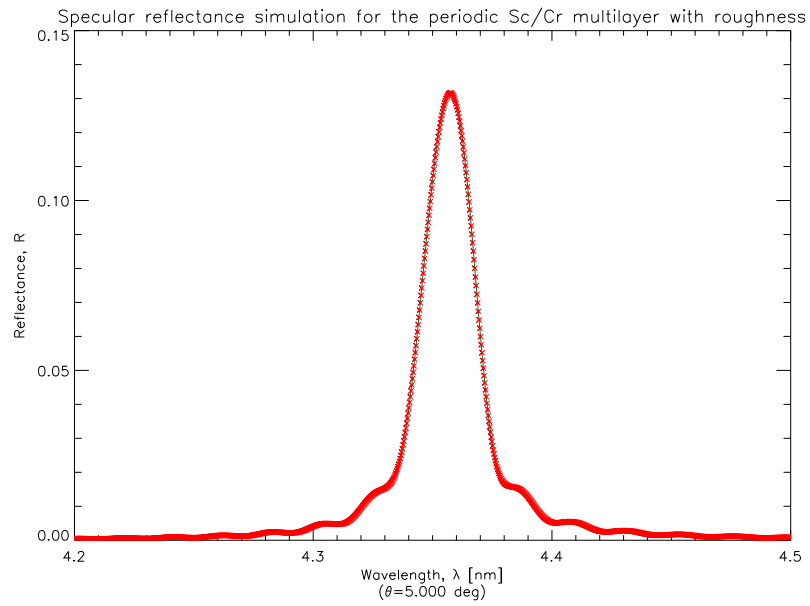


Figure 10: Specular reflectivity of a periodic 200-bilayer Sc/Cr multilayer with interface roughness of 0.3 nm at a fixed incidence angle of  $5^\circ$  from the normal.

## Interface Diffusion

The reflectivity simulations of two periodic Mo/Si multilayers with the same number of bilayers, period and Mo-to-Si ratio were compared in Figure 11. The only difference is that one takes into account interface diffusion by adding MoSi<sub>2</sub> interfacial layers and the other does not.

From Figure 11, the two reflectivity responses are similar except that the one with interface diffusion has a lower peak reflectivity.

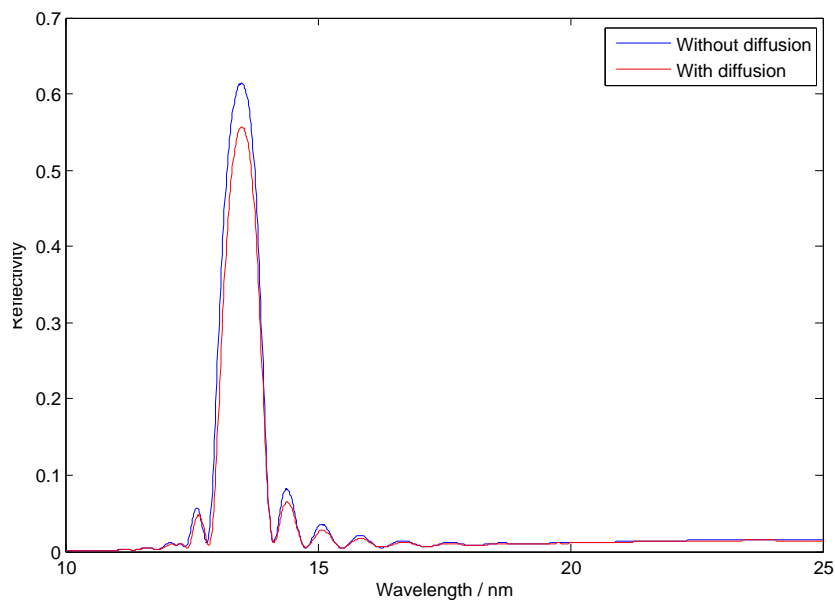


Figure 11: Specular reflectivity simulations for periodic Mo/Si multilayers with a fixed incidence angle of 5° from the normal ( $N = 20$ , period = 7.0 nm, Mo-to-Si ratio = 1:1)

## Interface Roughness

The reflectivity simulations of three periodic Sc/Cr multilayers with the same number of bilayers, period, Sc-to-Cr ratio but different rms roughness values are given in Figure 12. From this, it can be seen that a small increase in roughness results in a large decrease in the peak reflectivity.

Overall, all interfacial imperfections lead to the resultant loss of the reflectivity.

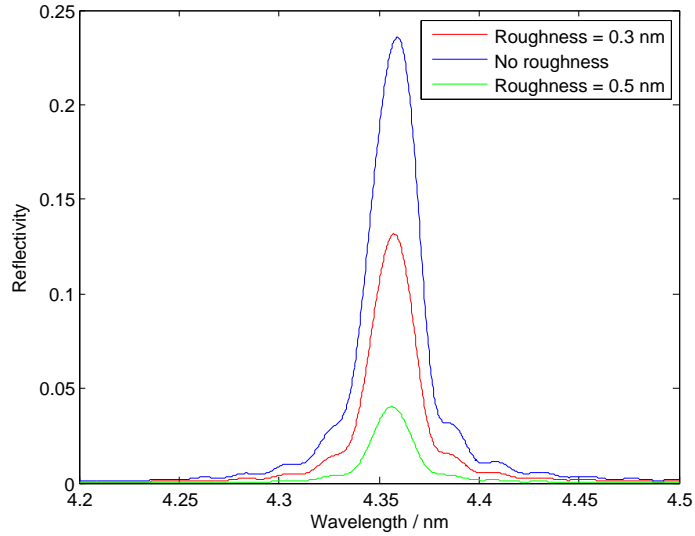


Figure 12: Specular reflectivity simulations for periodic Sc/Cr multilayers with three different degrees of interfacial roughness at a fixed incidence angle of  $5^\circ$  from the normal ( $N = 200$ , period = 2.2 nm, Sc-to-Cr ratio = 1:1)

## 4.3 Optimisation Results

### 4.3.1 Molybdenum/Silicon Multilayer System

The Mo/S aperiodic multilayer with  $N = 20$  was optimised for a top-flat broadband reflectivity between 17 and 22 nm at a fixed incidence angle of  $5^\circ$ . The optimisation design is shown in Figures 13 and 14.

### 4.3.2 Scandium/Chromium Multilayer System

The Sc/Cr aperiodic multilayer with  $N = 200$  was optimised for a top-flat broadband reflectivity between 4.30 and 4.42 nm at a fixed incidence angle of  $5^\circ$ . The optimised design is shown in Figures 15 and 16.

## 4.4 Comparison with Measurements

### 4.4.1 Hard X-ray Diffraction Measurements

An aperiodic Mo/Si multilayer was fabricated according the optimised design and characterised by the lab-based X-ray diffractometer as detailed in Section



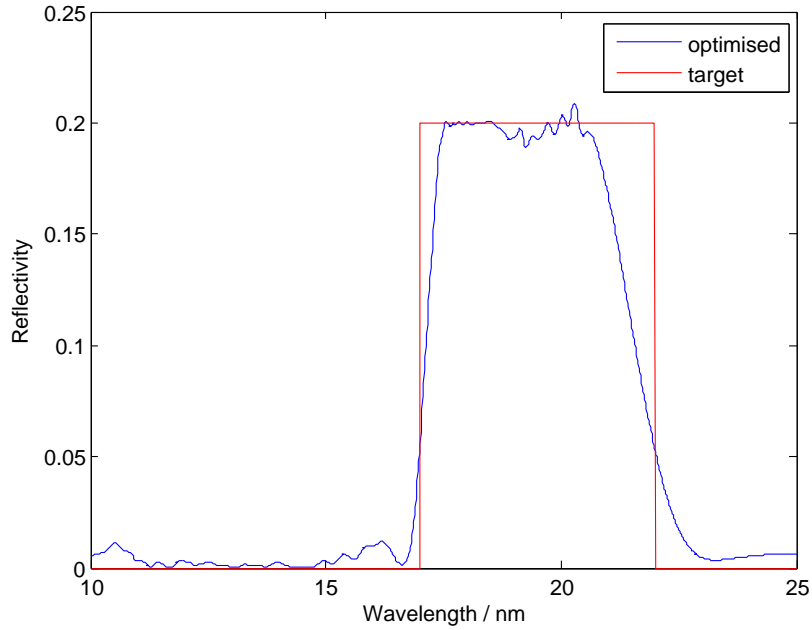


Figure 13: Specular reflectivity of the optimised aperiodic Mo/Si multilayer with  $N = 20$  at a fixed incidence angle of  $5^\circ$  from the normal.

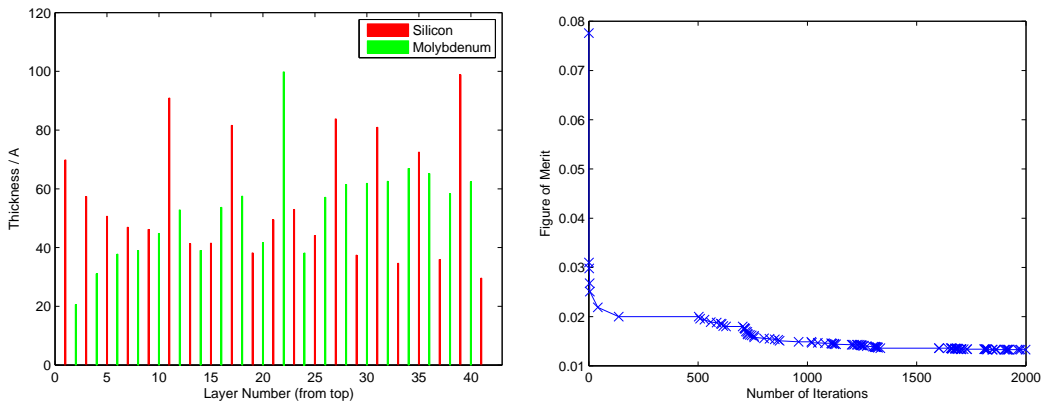


Figure 14: Thickness profile of the optimised aperiodic Mo/Si multilayer (left) and reduction of the figure of merit (right)

subsec:fab.

X-ray diffraction (XRD) measurements of the fabricated structure at a photon energy of 8 keV are shown in Figure 17 together with the XRD simulation for the optimised design.

The measured diffraction pattern was renormalised was such that the peak reflectance at around  $0.5 - -0.7^\circ$  grazing incidence angle coincides with

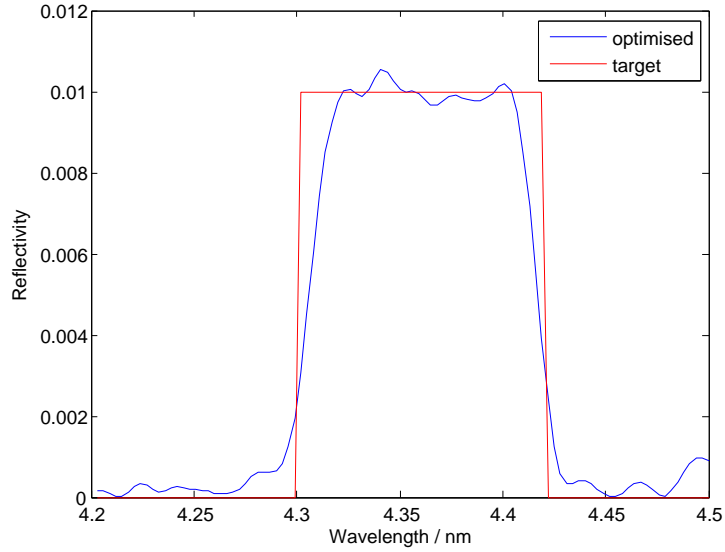


Figure 15: Specular reflectivity at of the optimised aperiodic Sc/Cr multilayer with  $N = 200$  at a fixed angle of incidence of  $5^\circ$  from the normal.

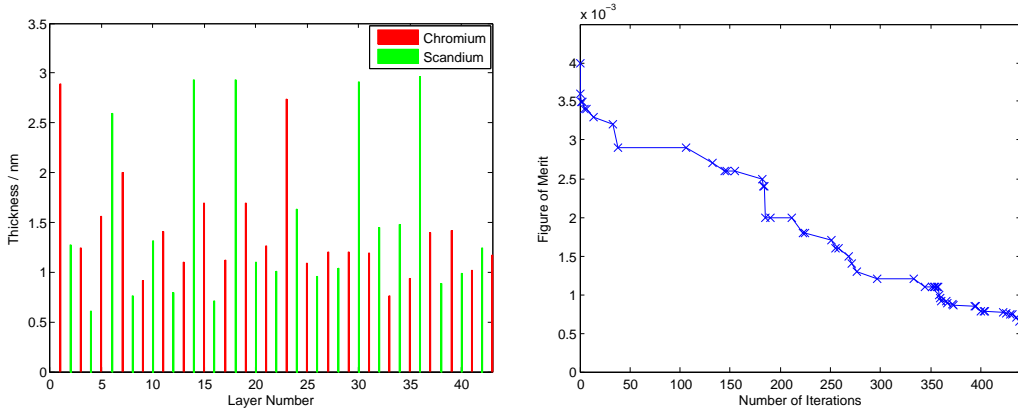


Figure 16: Thickness profile of the optimised aperiodic Sc/Cr multilayer (left) and reduction of the figure of merit (right)

the peak in the simulation. The agreement between these two plots is very good. They have the same overall shape except that one is slight shifted sideways. Note that the XRD measurements below about  $0.2 - -0.3^\circ$  show a significant deviation from the simulation. This comes from the fact that the incident beam is cut in half by the substrate at  $0^\circ$ .

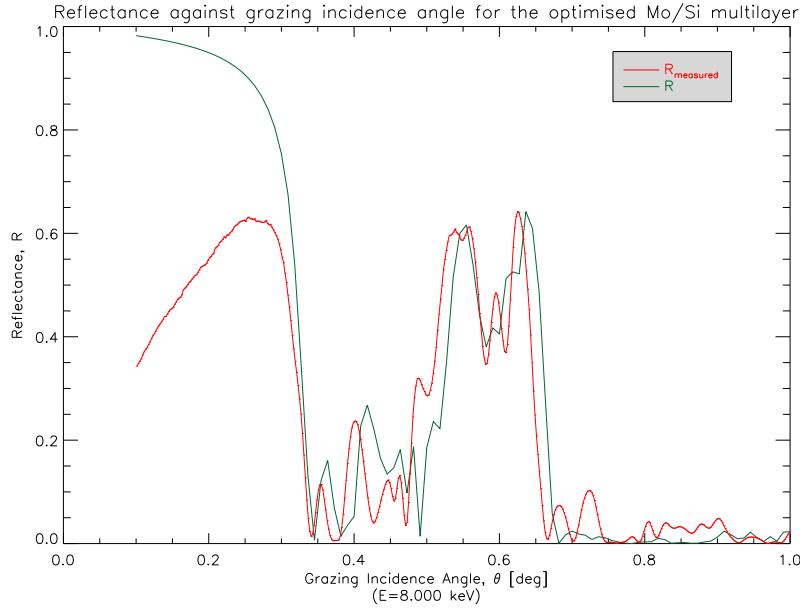


Figure 17: XRD measurements. The result for the fabricated Mo/Si multilayer is shown in red and the simulation for the optimised Mo/Si design is shown in green

#### 4.4.2 Soft X-ray Reflectivity Measurements

The previous result of a broadband aperiodic Sc/Cr multilayer with  $N = 100$  at an incidence angle of  $45^\circ$  is shown in Figure 18.

It was aimed to replicate this reflectivity profile using the codes we developed. The optimised reflectivity response is given in Figure 19. The replication was achieved successfully and we have an aperiodic Sc/Cr design with the reflectivity profile similar to that in Figure 18.

## 5 Further Discussions

### 5.1 Potential Applications

#### Ultrashort Soft X-ray Pulses

From the fourier transform, pulses that are extremely short in the time domain have a very large bandwidth in the wavelength or energy domain.

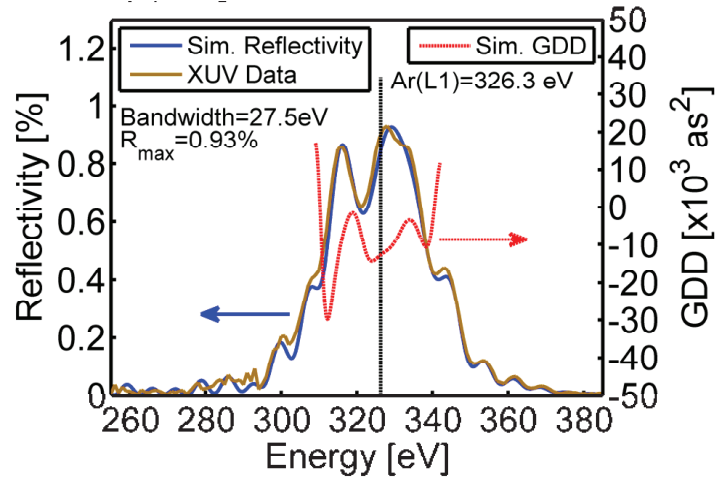


Figure 18: Previous work by Alexander Guggenmos showing a broadband reflectivity of about 1 %

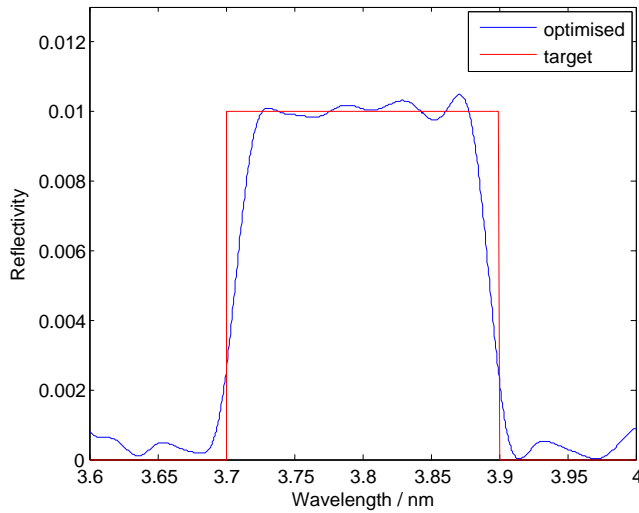


Figure 19: Soecular reflectance at of the optimised aperiodic Sc/Cr multilayer with  $N = 100$  at an incidence angle of  $45^\circ$ .

Hence, in order to work with these ultrashort soft X-ray pulses (order of  $10^{-12} - 10^{-15}s$ ), we need optical components with a large bandwidth in the soft X-ray region. Hence, broadband aperiodic soft X-ray multilayers are very suitable for this purpose.

## X-ray Imaging Systems

A large bandwidth is usually preferable in imaging systems as this will enable them to image a wide range of objects. Therefore, broadband aperiodic multilayers can be used as the optics for these systems.

### 5.2 Improvements to the Program

At the time of writing, the optimisation parameters, such as the wavelength range, the desired reflectivity response, the number of bilayers and the angle of incidence, were entered by directly editing the script codes. This can be inconvenient for general users who might prefer not to make corrections to the script codes. So the user interface can be developed for this purpose. This paper concerns more with the algorithm and the optimisation results.

From the performance aspects, The optimisation procedure could be improved by considering the following:

**Initial Parent Structure** It has been found that approximate analytic solutions can be found for two-component systems. These could be used as initial multilayer structures in the optimisation scheme, which would potentially reduce the computation time and increase the convergence rate significantly.

**Optimisation Scheme** There is a great variety of numerical optimisation methods. The Luus-Jaakola algorithm was chosen mainly because it is straightforward and easy to code but, at the same time, very effective.

## 6 Conclusions

1. Computational codes based MATLAB were developed to solve the inverse problem of finding the layer thicknesses for an aperiodic multilayer given a target reflectivity response.
2. In the Mo/Si system, the interfaces between materials can be treated as being purely diffuse. On the other hand, in the Sc/Cr system, the interfaces can be treated as being purely rough.
3. Taking into account the interfacial imperfections, the optimised aperiodic Mo/Si multilayer with 20 bilayers can achieve a bandwidth of

about 5 nm and a peak reflectivity of about 20 % at a fixed incidence angle of  $5^\circ$ . The optimised aperiodic Sc/Cr multilayer with 200 bilayers can achieve a bandwidth of about 0.12 nm and a peak reflectivity of about 1 % at a fixed incidence angle of  $5^\circ$ .

4. According to X-ray diffraction measurements, the deposition process used is able to fabricate an aperiodic Mo/Si multilayer according to the optimised design to very high accuracy.